Colloid Polym Sci (2008) 286:721–727
DOI 10.1007/s00396-007-1825-3

ORIGINAL CONTRIBUTION

Study of nylon 66–clay nanocomposites via condensation polymerization

Lei Song · Yuan Hu · Qingliang He · Fei You

Received: 13 July 2007 / Revised: 27 September 2007 / Accepted: 5 December 2007 / Published online: 5 January 2008

Abstract Nylon 66–clay (polyamide 66 (PA66)–organophilic montmorillonite (OMT)) exfoliated nanocomposites were synthesized based on nylon 66 salt and organoclay (OMT) modified by hydro-aminocaproic acid via condensation polymerization. And the nanocomposites were characterized by X-ray diffraction and transmission electronic microscopy. Exfoliated morphology with different clay content was obtained. The effects of cation exchange capacity and organic modified agent of OMT on the formation of exfoliated nanocomposites were investigated. It was shown that only suitable cation exchange capacity and organic modified agent could result in the formation of exfoliated morphology under the condition of condensation polymerization. The thermal and flammability properties of the nanocomposites were investigated through thermogravimetry and cone calorimetry experiments. Results indicate that the exfoliated nanocomposites have enhanced thermal stability and flame retardant properties compared with pure PA66.

Keywords Synthesis · Nylon 66 · Nanocomposites · Organoclay · Flame retardant

Introduction

In the past 20 years, polymer–clay nanocomposites have attracted great interest from many researchers because they frequently represent the improved or new properties compared with the pure polymer [1–10].Incorporation of a small quantity of nanoscale clay (<5 wt.%), the mechanical, thermal, dimensional, barrier, and flame retardant properties of the nanocomposites are improved significantly [2–10]. The enhanced properties of these nanocomposites are probably derived from the formed nanoscale structure, the large aspect ratio and large surface area of the clay layers, and the strong interaction between polymer molecular chains and clay layers. The studies of the flame retardant properties of the nanocomposites mainly demonstrate a significant decrease in the heat release rate (HRR), a change in the char structure, and a decrease in the mass loss rate (MLR) during combustion in a cone calorimeter [6–10]. The adsorption and wetting properties of hydrophobic or partially hydrophobic layer silicates have been well studied in recent years [11–14].

Nylon 66 (polyamide 66 (PA66)) is a kind of important engineering plastic in the family of nylon which is widely used in many fields. Some studies on nylon 66–organoclay nanocomposites have been reported via melt blending method [15–30]. The studies on the preparation [15, 16], hydrogen bonding [17], crystallization behavior [18–25], thermal stability and flammability [26, 27], mechanical properties [28–30], and morphology [15–30] of PA66–organoclay were reported. But there are few reports on PA66–organoclay nanocomposites via condensation polymerization method. In this article, we report the synthesis of PA66–organoclay nanocomposites via condensation polymerization method. The effects of cation exchange capacity and organic modified agent of organophilic montmorillonite (OMT) on the formation of nanocomposites are discussed. And the morphology, thermal stability, and flame retardant properties are investigated.

L. Song (✉) · Y. Hu · Q. He · F. You
State Key Lab of Fire Science,
University of Science and Technology of China,
Hefei, Anhui 230026, People's Republic of China
e-mail: leisong@ustc.edu.cn

Experimental

Materials

MMT1 (sodium montmorillonite (MMT), with a cation exchange capacity of 96 mmol/100 g, average particle size about 2 μm), MMT2 (sodium montmorillonite, with a cation exchange capacity of 122 mmol/100 g, average particle size about 2 μm), OMT1, and OMT2 were kindly provided by Ke Yan Company. Hereinto, OMT1 and OMT2 with a size of an average particle size about 2 μm were prepared from MMT1 and MMT2 by ion exchange reaction respectively, using hexadecyl trimethyl ammonium bromide (C16) in water solution according to the reported method [2]. The original MMT was gradually added to a previously prepared solution of hexadecyl trimethyl ammonium bromide (C16), which was dissolved in hot distilled water at 80 °C, and this suspension of MMT was stirred vigorously for 1 h. The precipitate was filtered and washed repeatedly with hot deionized water several times to remove the residue of C16. The product was placed in a vacuum drying oven at 80 °C for 12 h. The dried product was ground and screened to an average particle size of about 2 μm to obtain the end product, namely OMT which was modified with C16. This procedure was used to prepare OMT1 from MMT1 and OMT2 from MMT2.

6-Aminocaproic acid and nylon salt were purchased from Shanghai Ke Wang Chemical Reagents and Instruments Company and China ShenMa Group Co., Ltd., respectively. All the reactants and solvent were of analytical or chemical grade and were used without purification. Nylon 66 salt was synthesized from the reaction of adipic acid and hexamethylendiamine.

Preparation of OMTA1 and OMTA2

6-Aminocaproic acid, 6.55 g, diluted hydrochloric acid, 18.25 ml (10 wt.%), and distilled water, 200 ml, were placed in a 100-ml beaker. This solution was heated at 80 °C. Original montmorillonite, 16 g, was dispersed in 500-ml heated distilled water at 80 °C. This dispersion of MMT1 was added to the ammonium salt of the aminocaproic acid solution, and the resultant suspension was stirred vigorously for 30 min. The treated montmorillonite, a white precipitate, was isolated by filtration and washed repeatedly with hot deionized water several times. The product was placed in a vacuum drying oven at 80 °C for 12 h. Finally, the dried product was ground and screened to an average particle size of about 2 μm to obtain the end product, namely organophilic montmorillonite which was modified with hydro-aminocaproic acid. This procedure was used to prepare OMTA1 from MMT1 and OMTA2 from MMT2.

Synthesis of PA 66/OMTA1 and PA 66/OMTA2 hybrids

Nylon 66 salt, OMTA1, and acetate acid solution of hexamethylendiamine (used as controlled agent of molecular weight) were mixed and pestled together in a mortar and then the mixture was added in a closed container under flowing N_2 gas. The mixture was prepolymerized at 220–230 °C for 3 h. Then the temperature was continuously increased to 260–270 °C in 1.5 h. The prepolymer was polymerized for 1.5 h at 270 °C under normal pressure, then polymerized for 2 h under vacuum supply to decrease the water-liberated content during the polymerization. Finally, the product was poured into a flat mold under flowing N_2 gas and placed in a vacuum oven to cool to room temperature. The product was PA66–OMTA1 hybrid. The same procedure was used to synthesize PA66–OMTA2, PA66–OMT1 and PA66–OMT2 hybrids.

Measurement of molecular weight

The nanocomposites were extracted using formic acid with purity of 99.9% at room temperature and repeatedly filtered to ensure the removal of the clay, and then the molecular weights were determined by Ubbelohde viscosity method. A condensation polymerization of nylon 66 was carried out at the same time that the hybrids were synthesized, using the same procedure except for the absence of the clay. The viscosity average molecular weight (Mv) of the extracted polymers from all hybrids and from the pure nylon 66 was in the range of 11,000–12,000 which is lower than the commercial product.

Characterization

X-ray diffraction (XRD) experiments were performed directly on the samples using a Japan Rigaku D/max-rA X diffractometer (30 kV, 10 mA) with a Cu (λ=1.54Å) irradiation at the rate of 2 °/min in the range of 1.5–10 °. The samples for transmission electron microscopy (TEM) were cut from epoxy blocks with the embedded samples at room temperature using an ultramicrotome (Ultracut-1, UK). Thin specimens, 50–80 nm, were collected in a trough filled with water and then placed on 200-mesh copper grids. TEM images were obtained with a Hitachi H-800 microscope at an acceleration voltage of 100 kV. The thermogravimetric analyses (TGA) of samples were carried out under N_2 atmosphere with NETZSCH STA409C thermal analyzer from 50 °C to 800 °C at a heating rate of 15 °C/min. Cone calorimeter experiments were performed following the procedure defined in ISO 5660, on the 3-mm-thick 100×100 mm^2 plaques, using the cone-shaped heater. Heat release rate, mass loss rate, and specific

extinction area were obtained from the cone calorimetry experiment using online software. Typical results from cone calorimeter were reproducible within 10% at a heat flux of 35 kW/m^2.

Result and discussion

Formation mechanism of PA66 hybrids

Figure 1a,b shows the XRD patterns of the MMT1, MMT2, OMT1, OMT2, OMTA1, OMTA2, PA66/OMT1, PA66/OMT2, PA66/OMTA1, and PA66/OMTA2. And Table 1 lists all the XRD data of the samples. The average basal spacing (d_{001}) of MMT1 is 1.45 nm. Because the hydrophilic property and narrow galleries of MMT prevents the organic molecules intercalating the galleries of MMT, MMT should be modified by organic modified agent. In this paper, MMT1 was modified with two kinds of organically modified agent (C16 and hydro-aminocaproic acid) via cation exchange reaction to obtain two kinds of OMT (OMT1 and OMTA1). C16 and hydro-aminocaproic acid can displace Na^+ in the gallery of MMT. The average basal spacing (d_{001}) of OMTA1 modified with hydro-aminocaproic acid and OMT1 modified with C16 are 1.54 and 2.16 nm, respectively. When MMT was modified with organically modified agent, the galleries of MMT are intercalated and expanded by molecular chains of organically modified agent. The hydrophobic property and wide galleries of OMT are in favor of organic molecules intercalating the galleries of OMT.

After OMT1 have been heated at 220 °C for 1 h, Fig. 1a shows that the basal spacing (d_{001}) of OMT1 is decreased from 2.18 to 1.45 nm. It is shown that C16 degrades completely at that temperature. Thermal degradation of OMT begins at about 200°C and proceeds according to the Hoffman degradation mechanism [5]. In Fig. 1b, PA66–OMT1 shows d_{001} is about 1.45 nm, which indicates C16 of OMT1 degrades completely; OMT1 return to MMT1 so that the macromolecules of PA66 cannot accommodate in the galleries of hydrophilic MMT1.

PA66/4 wt.% OMTA1 and PA66/7 wt.% OMTA1 correspond to 4 and 7 wt.% contents of OMTA1 in the PA66 hybrids. XRD patterns of PA66/4 wt.% OMTA1 and PA66/7 wt.% OMTA1 show no (001) plane diffraction peak, which means a formation of exfoliated morphology. The TEM for PA66/7 wt.% OMTA1 (Fig. 2) also confirms that exfoliated morphology has been formed in the PA66 matrix. Individual silicate layers are well dispersed (Fig. 2). The XRD and TEM results both confirm that the exfoliated PA66–OMTA1 nanocomposites are obtained.

For the series of samples based on MMT2, the basal spacing (d_{001}) of MMT2 is 1.32 nm, and MMT2 was modified with C16 and hydro-aminocaproic acid to obtain OMT2 and OMTA2, respectively. d_{001} of OMTA2 and OMT2 are 1.37 and 2.08 nm. d_{001} of PA66/OMT2 is about 1.33 nm which indicates OMT2 cannot form intercalated or exfoliated morphology in the PA66 matrix the same as OMT1. C16 of OMT2 degrades completely at high temperature, OMT2 returns to MMT2 so that the macromolecules of PA66 cannot accommodate in the galleries of hydrophilic MMT2.

PA66/4 wt.% OMTA2 and PA66/7 wt.% OMTA2 correspond to 4 and 7 wt.% contents of OMTA2 in the PA66 matrix. Figure 1b shows that PA66/4 wt.% OMTA2 and PA66/7 wt.% OMTA2 have an obvious (001) plane diffraction peak at 4.16 ° and 4.27 °, respectively. This indicates d_{001} of PA66/4 wt.% OMTA2 and PA66/7 wt.% OMTA2 increases by 0.76 and 0.71 nm respectively, compared with that of OMTA2. These increases are indistinctive. TEM image (Fig. 2b) for PA66/7 wt.% OMTA2 shows a poor dispersion of OMTA2 particles

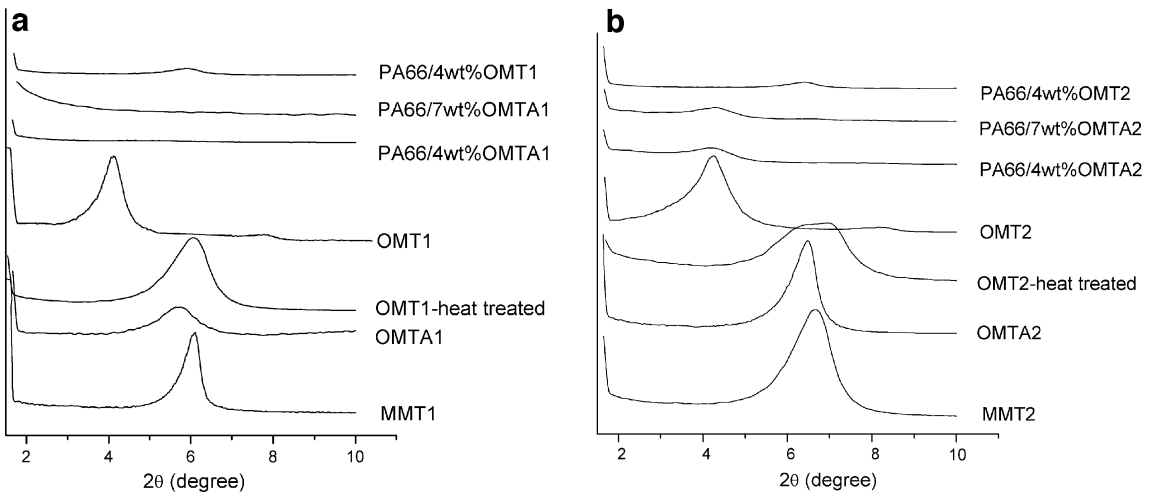

Fig. 1 XRD patterns of **a** series of samples based on MMT1 and **b** series of samples based on MMT2

Table 1 The XRD data of samples

Sample	2θ (°)	*d* (nm)	Sample	2θ (°)	*d* (nm)
MMT1	6.1	1.45	MMT2	6.7	1.32
OMTA1	5.75	1.54	OMTA2	6.45	1.37
OMT1	4.1	2.18	OMT2	4.25	2.08
OMT1-heat treated	6.1	1.45	OMT2-heat treated	6.5	1.35
PA66/4 wt.% OMTA1	<1.5	Exfoliated	PA66/4 wt.% OMTA2	4.16	2.13
PA66/7 wt.% OMTA1	<1.5	Exfoliated	PA66/7 wt.% OMTA2	4.27	2.08
PA66/4 wt.% OMT1	6.1	1.45	PA66/4 wt.% OMT2	6.41	1.33

containing many silicate layers. Therefore, XRD and TEM results confirm PA66–OMTA2 hybrids are not nanocomposites, its structures are more close to microcomposites.

The formation of the different morphology of PA66–OMTA1 and PA66–OMTA2 are explained by the following mechanism.

MMT1 and MMT2 are two kinds of Na^+ montmorillonite with the different cation exchange capacity, 96 and 122 mmol/100 g, respectively. It is indicated that the layer charge density of MMT1 is lower than that of MMT2. Although the cation exchange capacity of MMT2 is larger than that of MMT1, the basal spacing of MMT2, OMT2, and OMTA2 is less than the corresponding MMT1, OMT1, and OMTA1. The selective liquid sorption properties of the hydrophobized silicate surfaces are the key factor at the organic molecule intercalation. The previous studies [3] reported that the layer charge density of clays mediates the amount of monomer that can diffuse in the intragallery region. The low layer charge density clay is in favor of forming OMT with a lateral bilayer of modified agent and the high layer charge density clay is in favor of forming OMT with a monolayer of modified agent. The clay with low-to-intermediate layer charge densities is best suited for the formation of exfoliated nanocomposites. The reason probably is that the larger layer charge density leads to the larger polarity and the larger electrostatic force between the layers. Dekany et al. [13, 14] studied the liquid adsorption and immersional wetting properties of the hydrophobic layered silicates with different surface hydrophobicity on the respect of the thermodynamic analysis. They found that the organophilic montmorillonite has two adsorption regions of different energies occurring at the layer surface and the long hydrophobic alkyl chains attached at the layer surface. The interlayer alkyl chains are solvated by the nonpolar group of the intercalated organic molecule and the silicate surface not covered by alkyl chains is solvated by the polar group of intercalated organic molecule [11, 12]. In this study, the hypothesis illustrated in Fig. 3 summarizes the formation mechanisms of PA66–OMTA1 and PA66–OMTA2 hybrids.

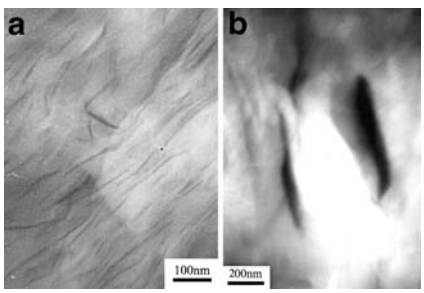

Fig. 2 The TEM images of **a** PA66/7 wt.% OMTA1 nanocomposite and **b** PA66/7 wt.% OMTA2 hybrid

For OMTA1, the layer charge density is correspondingly low; the population density of organic modified agent in the intragallery of OMTA1 is corresponding low, so the free volume in the intragallery is corresponding large. The arrangement of organically modified agent, namely, hydro-aminocaproic acid molecules may be bilayer in the intragallery of OMTA1. The layer surface not covered by organically modified agents and the free volume in the intragallery of OMTA1 is correspondingly large, and the monomer is well compatible with hydro-aminocaproic acid molecules and silicate surface which is a kind of organic salt. So there is a correspondingly large amount of monomer intercalate in the intragallery of OMTA1. In the prepolymerization process, the melted monomer (nylon 66 salt) can easily diffuse the intragallery of OMTA1 and then take prepolymerization to obtain solid prepolymer (dimer, trimer, and tetramer) in the prepolymerization process. Simultaneously, the grafting reaction between the carboxyl group of hydro-aminocaproic acid and the amino group of monomer molecules lets some monomer molecules graft on the layers in the intragallery of OMTA1, namely the molecule chains of the organically modified agent of OMTA1 become longer, so that the long molecule chains of the organically modified agent are well compatible with more prepolymer molecules. Because of the reactions including prepolymerization and grafting reaction, the gallery of OMTA1 becomes wide and compatible enough to accommodate the larger prepolymer molecules in the condensation polymerization process. Consequently, the melted prepolymer can easily diffuse the widening gallery of OMTA1 and take reactions including polymerization and grafting reaction. The gallery of OMTA1 becomes wide and compatible enough to accommo-

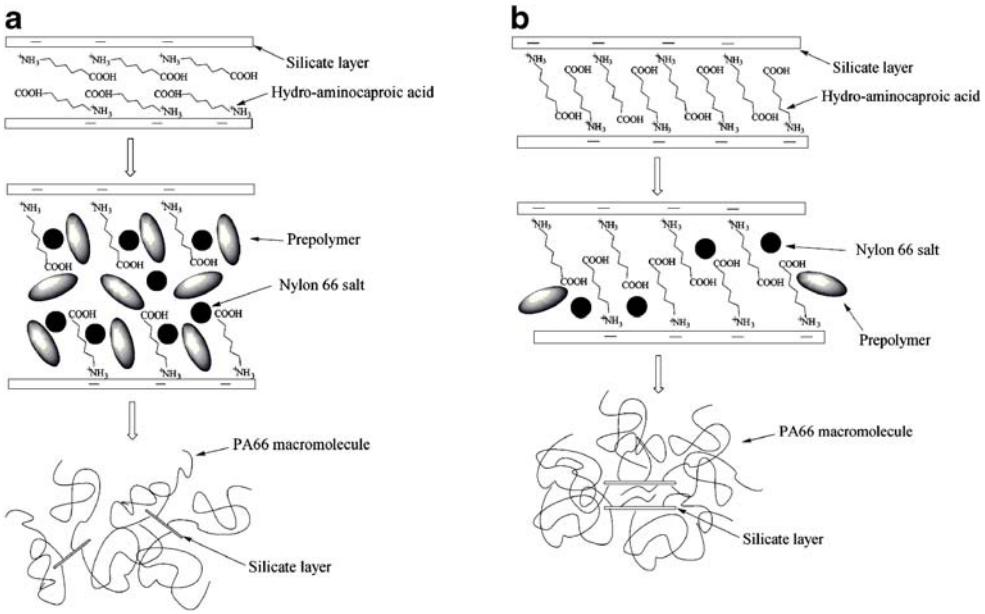

Fig. 3 **a** Proposed formation mechanism of PA66–OMTA1; **b** Proposed formation mechanism of PA66–OMTA2

date more prepolymer molecules to feed this diffusion–reaction–expansion process, until the OMTA1 layers are fully exfoliated. XRD and TEM results confirm that the exfoliated nanocomposites are obtained.

For OMTA2, the layer charge density and the amount and population density of organically modified agent (hydro-aminocaproic acid) are higher than that of OMTA1. The arrangement of hydro-aminocaproic acid molecules in the intragallery of OMTA2 is monolayer which is different from OMTA1. Therefore, the spatial hindered effect of OMTA2 on the monomer diffusing intragallery is higher than that of OMTA1. Moreover, the layer surface not covered by organic modified agents and the free volume in the intragallery of OMTA2 is correspondingly low, which is also unfavorable for the monomer intercalation. In prepolymerization process, the amount of melted monomer which can diffuse the intragallery of OMTA2 is less than that of OMTA1 because of the stronger spatial hindered effect and smaller free volume and layer surface not covered by organically modified agents. Instead, quite a few monomers which were hindered outside the galleries of OMTA2 can take the graft reaction with the hydro-aminocaproic acid molecules grafted at the edge of OMTA2 layers. In the intragallery, the monomer also can take reactions including prepolymerization and grafting reaction. But the amount of monomer which can diffuse the intragallery is not enough to cause the gallery to become wider and more compatible to accommodate more extragallery prepolymer molecules in the polymerization process. Along with the condensation polymerization proceeding, the OMTA2 layers are encapsulated by polymer molecules grafted on the edge of the layers, which also insulate the intragallery of OMTA2 from melted extragallery polymer molecules intercalating. So there are a few oligomer formed in the intragallery of OMTA2. XRD patterns show that d_{001} of PA66/4 wt.% OMTA2 and PA66/7 wt.% OMTA2 are 2.13 and 2.08 nm, respectively. It is indicated that monomer intercalate the gallery of OMTA2 and cause the gallery to widen in the prepolymerization process; the prepolymer molecules can hardly intercalate the gallery of OMTA2 in polymerization process because the increase of gallery is not exceeding 1 nm; the intragallery reaction cannot cause OMTA2 exfoliation. Moreover, the OMTA2 particle which is isolated by PA66 macromolecules cannot be cleaved to smaller primary particles.

In summary, the influence factors on formation of exfoliated morphology via condensation polymerization include several key functions of the nature of montmorillonite, the compatibility between the organic agents of OMT and polymer matrix, the spatial hindered effect of the organic agents of OMT, and the chemical reactions between the organic agents and polymer.

Thermal stability

The TGA results of PA66, PA66/4 wt.% OMTA1, PA66/7 wt.% OMTA1 and PA66/4 wt.% OMTA2 are shown in Fig. 4 and Table 2.

In regard to pure PA66, the degradation temperature at 320–480 °C is attributed to the depolycondensation and cross-linking reaction [31]. Then at higher temperature, the material degrades slowly and leaves 4.18 wt.% stable char residue at 780 °C. In the presence of OMTA1, the enhanced effect of OMTA1 on the thermal stability is obvious; the degradation of PA66 hybrid begins at a higher temperature. $T_{5\%}$ (the degradation temperature of 5% weight loss) of

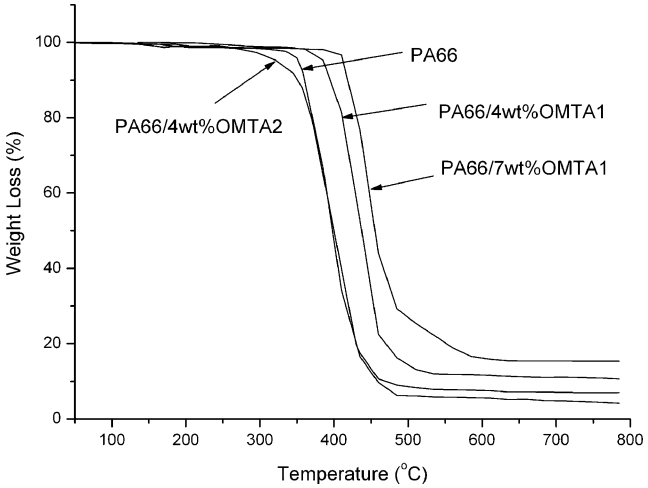

Fig. 4 TGA curves of PA66–OMTA1 and PA66–OMTA2 samples

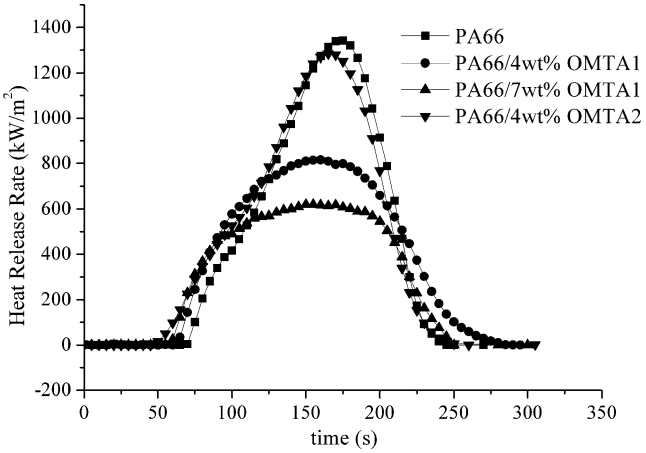

Fig. 5 Plot of heat release rate of PA66–OMTA1 and PA66–OMTA2 samples

PA66/4 wt.% OMTA1 and PA66/7 wt.% OMTA1 increases compared with that of pure PA66 along with the content of OMTA increase. The weight percents of char residue of samples at 780 °C are shown in the TGA curves and listed in Table 2. The weight percent of char residue increases along with the content of OMTA1 increase. The incorporation of OMTA1 enhances the thermal stability and carbonaceous char formation of PA66 hybrid derived from the barrier effect of nanoscale OMTA1 layers. For PA66/4 wt.% OMTA2, TGA results show that $T_{5\%}$ is much lower than that of pure PA66. It is indicated that the presence of OMTA2 decreases the thermal stability of PA66 hybrid. The reason probably is that the thermal stability of oligomers in the intragallery of OMTA2 is correspondingly low which degrades at lower temperature compared with the pure PA66. This indirectly confirmed the above hypothetical formation mechanism.

Flame retardant properties

HRR was measured by cone calorimeter; HRR peak (pHRR) was found to be the most important parameter to evaluate fire safety. Figure 5 shows that pure PA66 burns very fast after ignition and reaches a sharp peak on the HRR curve, whereas the loading of OMTA1 results in a great decline of HRR. PA66/4 wt.% OMTA1 and PA66/7 wt.% OMTA1 have 39% and 54% lower HRR than the pure PA66. Addition of 4 wt.% content of OMTA2 only causes the pHRR decreasing about 4%. It is shown that OMTA1 has a significant flame retardant property derived from nanoscale barrier effect, but OMTA2 does not show obvious flame retardant effect. Some data measured by cone calorimetry are listed in Table 3 including the peak values of HRR, MLR, and special extinction area (SEA). For PA66–OMTA1, the less these values are, the less are the released amounts of heat and smoke. These data show some information as follows: the maximum values of HRR, MLR, and SEA decrease in the presence of OMTA1; when OMTA2 exist, these values almost do not change. These results show that the addition of OMTA1 reduces the amount of the flammable small decomposition products released during combustion. However, OMTA2 does not show obvious flame retardant property. Studies [6–10] suggest that the lower flammability of polymer–clay nanocomposites is due to the formation of a multilayered carbonaceous-silicate structure in the condensed phase. The lower cone values of nylon 66–OMT nanocomposites might be attributed to that barrier effect of nanoscale clay compared with combustion of pure nylon 66, which is shown in Fig. 5 and Table 3. The nylon 66–OMTA2 does not show this barrier effect of nanoscale clay. This also confirmed that the nylon 66/OMTA2 is not the nanocomposite but is the microcomposite.

Table 2 The TGA results of PA66 and PA66/OMT nanocomposites

Sample	$T_{5\%}$ (°C)	Residue at 780 °C (wt.%)
PA66	350	4.18
PA66/4 wt.% OMTA1	383	10.68
PA66/7 wt.% OMTA1	411	15.29
PA66/4 wt.% OMTA2	318	7.00

Table 3 Cone data of samples

Samples	Peak HRR (kW/m^2)	Peak MLR (g/m^2s)	Peak SEA (m^2/kg)
PA66	1,342	0.30	1,345
PA66/4 wt.% OMTA1	815	0.22	595
PA66/7 wt.% OMTA1	620	0.17	424
PA66/4 wt.% OMTA2	1,284	0.29	1,345

Conclusion

Exfoliated polyamide 66–organoclay (PA66–OMT) nanocomposites were synthesized based on nylon 66 salt and OMT modified by hydro-aminocaproic acid via condensation polymerization. X-ray diffraction and transmission electronic microscopy were used to confirm the exfoliated morphology formation. The effects of cation exchange capacity and organic modifier agent of OMT were investigated to discuss the formation mechanism of exfoliated nanocomposites. The low cation exchange capacity and reactive modified agent is in favor of forming exfoliated morphology under the condition of condensation polymerization. The intercalation and exfoliation processes are obviously affected by comprehensive effect of physical and chemical functions. And the exfoliated nanocomposites have enhanced thermal stability and flame retardant properties compared with pure PA66. The microcomposites does not show these enhanced thermal stability and flame retardant properties.

Acknowledgement The work was financially supported by the National Natural Science Foundation of China (No.50476026) and Specialized Research Fund for the Doctoral Program of Higher Education (20040358056).

References

1. Vaia RA, Ishii H, Giannelis EP (1993) Chem Mater 5:1694
2. Hu Y, Song L, Xu JY, Yang L, Chen ZY, Fan WC (2001) Colloid Polym Sci 279:819
3. Lan T, Kaviratna PD, Pinnavaia TJ (1995) Chem Mater 7:2144
4. Song L, Hu Y, Tang Y, Zhang R, Chen ZY, Fan WC (2005) Polym Degrad Stab 87:111
5. Xie W, Gao ZM, Pan WP, Hunter D (2001) Chem Mater 13:2979
6. Bourbigot S, Le Bras M, Dabrowski F, Gilman JW, Kashiwagi T (2000) Fire Mater 24:201
7. Bourbigot S, Devaux E, Flambard X (2002) Polym Degrad Stab 75:397
8. Gilman JW, Jackson CL, Morgan AB, Harris R, Manias E, Giannelis EP et al (2000) Chem Mater 12:1866
9. Zanetti M, Camino G, Canavese D, Morgan AB, Lamelas FJ, Wilkie CA (2002) Chem Mater 14:189
10. Tang Y, Hu Y, Wang SF, Gui Z, Chen ZY, Fan WC (2003) Polym Int 52:1396
11. Dekany I, Szanto F, Nagy LG (1986) J Colloid Interface Sci 109:376
12. Dekany I (1992) Pure and Appl Chem 64:1499
13. Dekany I, Szanto F, Weiss A, Lagaly G (1986) Ber Bunsenges Phys Chem 90:427
14. Marosi T, Dekany I, Lagaly G (1992) Colloid and Polymer Sci 270:1027
15. Liu XH, Wu QJ (2002) Macromol Mater Eng 287:180
16. Han B, Ji G, Wu S, Shen J (2003) Eur Polym J 39:1641
17. Lu YL, Zhang GB, Feng M, Zhang Y, Yang M, Shen D (2003) J Polym Sci B: Polym Phys 41:2313
18. Liu XH, Wu QJ, Berglund L (2002) Polymer 43:4967
19. Liu XH, Wu QJ, Zhang QX, Mo ZS (2003) J Polym Sci B: Polym Phys 41:63
20. Zhang QX, Yu ZZ, Yang MS, Ma J, Mai YW (2003) J Polym Sci B: Polym Phys 41:2861
21. Shen L, Phang IY, Chen L, Liu TX, Zeng KY (2004) Polymer 45:3341
22. Shen L, Phang IY, Liu TX, Zeng KY (2004) Polymer 45:8221
23. Lu YL, Zhang Y, Zhang GB, Yang MS, Yan SK, Shen DY (2004) Polymer 45:8999–9009
24. Kang X, He SQ, Zhu CS, Lu LWL, Guo JG (2005) J Appl Polym Sci 95:756
25. Hedicke K, Wittich H, Mehler C, Gruber F, Altstadt V (2006) Compos Sci Technol 66:571
26. Qin HL, Su QS, Zhang SM, Zhao B, Yang MS (2003) Polymer 44:7533
27. Phang IY, Chen L, Tjiu WC, Pisharath S, Liu TX (2004) Mater Res Innov 8:159
28. Yu ZZ, Yan C, Yang MS, Mai YW (2004) Polym Int 53:1093
29. Vlasveld DPN, Vaidya SG, Bersee HEN, Picken SJ (2005) Polymer 46:3452
30. Gyoo PM, Venkataramani S, Kim SC (2006) J Appl Polym Sci 101:1711
31. Levchik SV, Weil ED, Lewin M (1999) Polym Int 48:532